NAVAL POSTGRADUATE SCHOOL

MONTEREY, CALIFORNIA

THESIS

THE ROLE OF GENERATION VOLUME AND PHOTON RECYCLING IN "TRANSPORT IMAGING" OF BULK MATERIALS

by

Yoseph Seo

December 2011

Thesis Advisor:	Nancy M. Haegel
Second Reader:	Peter P. Crooker

Approved for public release; distribution is unlimited

THIS PAGE INTENTIONALLY LEFT BLANK

REPORT DOCUMENTATION PAGE			*Form Approved OMB No. 0704–0188*
Public reporting burden for this collection of information is estimated to average 1 hour per response, including the time for reviewing instruction, searching existing data sources, gathering and maintaining the data needed, and completing and reviewing the collection of information. Send comments regarding this burden estimate or any other aspect of this collection of information, including suggestions for reducing this burden, to Washington headquarters Services, Directorate for Information Operations and Reports, 1215 Jefferson Davis Highway, Suite 1204, Arlington, VA 22202–4302, and to the Office of Management and Budget, Paperwork Reduction Project (0704–0188) Washington DC 20503.			
1. AGENCY USE ONLY ***(Leave blank)***	**2. REPORT DATE** December 2011	**3. REPORT TYPE AND DATES COVERED** Master's Thesis	
4. TITLE AND SUBTITLE The Role of Generation Volume and Photon Recycling in "Transport Imaging" of Bulk Materials		**5. FUNDING NUMBERS**	
6. AUTHOR(S): Yoseoph Seo			
7. PERFORMING ORGANIZATION NAME(S) AND ADDRESS(ES) Naval Postgraduate School Monterey, CA 93943–5000		**8. PERFORMING ORGANIZATION REPORT NUMBER**	
9. SPONSORING /MONITORING AGENCY NAME(S) AND ADDRESS(ES) N/A		**10. SPONSORING/MONITORING AGENCY REPORT NUMBER**	
11. SUPPLEMENTARY NOTES: The views expressed in this thesis are those of the author and do not reflect the official policy or position of the Department of Defense or the U.S. Government. IRB Protocol number _____N/A_____.			
12a. DISTRIBUTION / AVAILABILITY STATEMENT Approved for public release; distribution is unlimited		**12b. DISTRIBUTION CODE**	

13. ABSTRACT (maximum 200 words)

The goal of this research was to use Monte Carlo simulations to further develop the model that describes transport imaging by including a more realistic description of the generation region created by the incident electrons. Monte Carlo simulation can be used to determine the energy distribution in bulk materials due to the interaction with incident electrons. In the simulation, the incident electrons undergo both elastic and inelastic scattering events. Through these events, the energy of the electrons is transferred to the target materials. This deposited energy can generate electron-hole pairs and then, via recombination, photons. In the experimental work, these photons are measured by a CCD camera connected to an optical microscope in a scanning electron microscope (SEM).

Monte Carlo simulations were performed for a range of target materials and compared to the luminescence distributions measured experimentally. The simulated energy distributions are always spatially narrower than the optical image from the SEM. We propose possible explanations that need to be evaluated: the relationship between deposited energy and final electron distributions in the target material and photon recycling, in which locally generated photons are reabsorbed to produce a wider luminescence distribution. Further experiments are proposed to identify the limiting factors determining the minimum luminescence distribution.

14. SUBJECT TERMS Nuclear detection system, transport imaging, Monte Carlo simulation, CASINO			**15. NUMBER OF PAGES** 49
			16. PRICE CODE
17. SECURITY CLASSIFICATION OF REPORT Unclassified	**18. SECURITY CLASSIFICATION OF THIS PAGE** Unclassified	**19. SECURITY CLASSIFICATION OF ABSTRACT** Unclassified	**20. LIMITATION OF ABSTRACT** UU

NSN 7540–01–280–5500 Standard Form 298 (Rev. 2–89)
Prescribed by ANSI Std. 239–18

THIS PAGE INTENTIONALLY LEFT BLANK

Approved for public release; distribution is unlimited

THE ROLE OF GENERATION VOLUME AND PHOTON RECYCLING IN "TRANSPORT IMAGING" OF BULK MATERIALS

Yoseoph Seo
Major, Republic of Korea Army
B.S., Korea Military Academy, 1999

Submitted in partial fulfillment of the
requirements for the degree of

MASTER OF SCIENCE IN COMBAT SYSTEMS TECHNOLOGY

from the

NAVAL POSTGRADUATE SCHOOL
December 2011

Author: Yoseoph Seo

Approved by: Nancy M. Haegel
Thesis Advisor

Peter Crooker
Second Reader

Andres Larraza
Chair, Department of Physics

THIS PAGE INTENTIONALLY LEFT BLANK

ABSTRACT

The goal of this research was to use Monte Carlo simulations to further develop the model that describes transport imaging by including a more realistic description of the generation region created by the incident electrons. Monte Carlo simulation can be used to determine the energy distribution in bulk materials due to the interaction with incident electrons. In the simulation, the incident electrons undergo both elastic and inelastic scattering events. Through these events, the energy of the electrons is transferred to the target materials. This deposited energy can generate electron-hole pairs and then, via recombination, photons. In the experimental work, these photons are measured by a CCD camera connected to an optical microscope in a scanning electron microscope (SEM).

Monte Carlo simulations were performed for a range of target materials and compared to the luminescence distributions measured experimentally. The simulated energy distributions are always spatially narrower than the optical image from the SEM. We propose possible explanations that need to be evaluated: the relationship between deposited energy and final electron distributions in the target material and photon recycling, in which locally generated photons are reabsorbed to produce a wider luminescence distribution. Further experiments are proposed to identify the limiting factors determining the minimum luminescence distribution.

THIS PAGE INTENTIONALLY LEFT BLANK

TABLE OF CONTENTS

THIS PAGE INTENTIONALLY LEFT BLANK

LIST OF FIGURES

LIST OF TABLES

THIS PAGE INTENTIONALLY LEFT BLANK

ACKNOWLEDGMENTS

This work was supported in part by the Domestic Nuclear Detection Office (DNDO) of the Department of Homeland Security under Interagency Agreement HSHQDC-11-X-00015.

I would like to thank the Republic of Korea Army for giving me this opportunity to study a master's course here at Naval Postgraduate School. I would also like to thank for all her support, my thesis advisor, Dr. Nancy Haegel. Without her mentorship, guidance and patience, I could not make my thesis completed. Dr. Peter Crooker also plays an important role in my research. His logical criticism made me think more about the research. In addition, I need to thank my colleague, Maj. Dave Phillips. He helped me to understand the important concepts and to provide experimental data for thallium bromide.

Finally, I would like to give a special thanks to my spouse, Soin, and my daughters, Yehyun and Eunhyun. They always give me support and encouragement.

THIS PAGE INTENTIONALLY LEFT BLANK

I. INTRODUCTION

A. SEMICONDUCTOR MATERIALS FOR NUCLEAR RADIATION DETECTION

In recent years, nuclear materials have been developed and used in many industries and in an increasing number of countries. However, the more radioactive materials are utilized, the more threats of uncontrolled use of radioactive materials the world has to confront. To minimize these threats, nuclear materials should be monitored, controlled, and easily identified. Therefore, it is crucial to develop an effective and efficient nuclear radiation detector. The future detector should be low-cost, operate efficiently at room temperature and be small and light to carry. For these reasons, scientists are now evaluating a wide range of new potential detector materials.

Semiconductors have good characteristics for a nuclear radiation detector. First, many semiconductors have a high atomic number Z. This is important because the higher the atomic number of a material, the higher the density. A material with higher density can stop electrons or photons more effectively in the same volume, so the material absorbs more energy from the source in the same volume. In addition, a semiconductor generates electron-hole pairs when these materials absorb photons with higher energy than the band-gap energy. The energy of nuclear radiation (~MeV) is usually much higher than the band-gap energy (~eV) of semiconductors and so a large number of electron-hole pairs are produced. The electron-hole pair products are converted to a current pulse from which one can determine the intensity and type of radiation.

Since semiconductors have a high atomic number Z and the potential to convert energy directly to electron-hole pairs, they are more compact and have better energy resolution than other detection methods. As a result, semiconductors are valuable for applications that require higher energy-resolution. This resolution is a result of the efficiency of transporting charge after absorption of radiation in the material. In the semiconductor detection system, the distribution of electron-hole pairs provides the spectral characteristics of detected radiation. In a semiconductor, the intensity of nuclear radiation is converted to a current by an applied electric field which transports the charge

to the contacts. To determine the relationship between the intensity of radiation and the current collected in a detector, the mobility-lifetime product of a semiconductor plays a key role. In Figure 1 and Figure 2, the spectra from a thallium bromide detector show the difference between radiation from 137-cesium and 57-cobalt. The value and uniformity of the mobility-lifetime product determine the quality of spectral resolution that can be obtained.

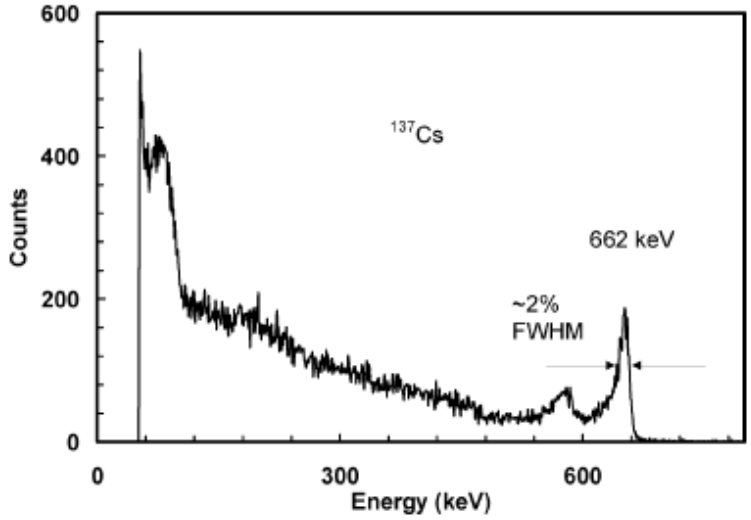

Figure 1 137-Cs pulse height spectrum recorded from one pixel of a 6.7 mm thick TlBr array. From [1].

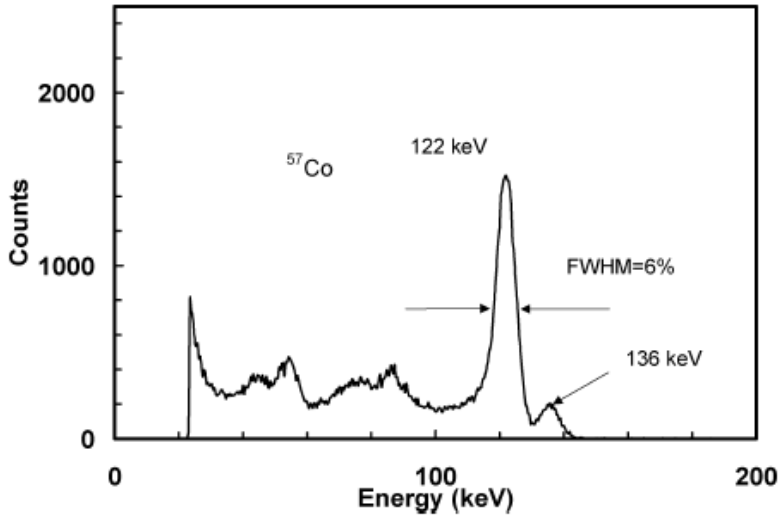

Figure 2 57-Co pulse height spectrum recorded from one pixel of a 10 mm thick TlBr array. From [1].

B. THE MOBILITY-LIFETIME ($\mu\tau$) PRODUCT

Mobility μ is the proportionality constant between the applied field E and the drift velocity $v = \mu E$. This is a measure of how easily an electron can move through a semiconductor in an applied electric field E. Electrons moving in a material travel a random path. During an electron's travels, there are elastic and inelastic scatterings that occur. The time between scattering events is the scattering or recombination lifetime (τ) of electrons. Both the mobility and the lifetime are intrinsic characteristics of a material and they determine the behavior of charge transport in semiconductors.

In a simple case, we consider a uniform volume excitation that generates free electrons. The magnitude of the current is proportional to $\mu\tau E$:

$$\mathrm{I} = (\mathrm{eF}/\mathrm{L})(\mu\tau E), \tag{1}$$

where I is the current, F is the generation rate of free carriers (pairs per second), L is the distance between detector electrodes, and E is the applied electric field. Thus, the $\mu\tau$ product indicates how well a semiconductor performs current collection for radiation detectors [2].

Traditionally, germanium and silicon are materials that have a good $\mu\tau$ product. However, the bandgaps of germanium and silicon are relatively small, 0.67 eV and 1.11 eV, respectively. This means that germanium and silicon have thermal currents at room temperature. To avoid thermal noise, these materials must be cooled. Therefore, a material with both a good $\mu\tau$ product and relatively high bandgap energy is needed to reduce cost and avoid the complexity of a cooling system.

C. DETERMINE $\mu\tau$ PRODUCT

The mobility-lifetime product is the key transport parameter of a material. Usually, this parameter is determined by an experimental method, one of which is "transport imaging." Transport imaging measures the spatial distribution of electron-hole pair recombination in a material in response to local excitation. This transport imaging can measure the $\mu\tau$ product in the material without contact by using an electron beam to generate charge and then imaging the resulting luminescence distribution. However, this

method is applied with the assumption that the diffusion length of free carriers in a material is larger than the generation volume. In experimental results, when the diffusion length is longer than ~ 10 microns, the generation volume could be ignored. Otherwise, the generation volume should be considered for measuring diffusion length of carriers in a material. Therefore, for relatively short diffusion length materials, understanding and measuring the generation volume is crucial. In this research, Monte Carlo simulation is the method used to determine the generation volume.

D. MILITARY RELEVANCE

Compact and efficient nuclear detectors are needed for locating, monitoring, or identifying radioactive materials [2]. A semiconductor detection system is one alternative for a compact and efficient detector. Through research and the use of novel materials, the volume and cost of nuclear radiation detectors can be reduced innovatively. Then the radiation detector can be combined with communication systems and unmanned systems, for broad deployment.

As a chemical, biological, radiological and nuclear (CBRN) officer in South Korean Army, the author operates several radiation detectors. With nuclear events, such as with nuclear power or nuclear explosive, the army needs many detectors having low cost and simple operation at room temperature. A room temperature semiconductor nuclear detection system will be the future goal for low-cost and simple detection system. This work can contribute to the characterization tools required to reach this goal.

II. TRANSPORT IMAGING

Transport imaging is the direct imaging of charge transport, which is obtained in semiconductors by combining the excitation capability and resolution of a scanning electron microscope (SEM) with an optical microscope [3]. In a SEM, an incident electron with an energy of 10, 20 or 30 keV can deposit energy in the material. Electrons in the target material move from the valence band to the conduction band making electron-hole pairs in the semiconductor. These charge carriers undergo random motion and spread out in the material. When electrons and holes meet, recombination occurs. In this recombination, electrons return from the conduction band to the valence band, losing energy equal to the band-gap energy. This process generates photons. These photons are captured by a Si-CCD camera attached to the optical microscope.

Transport imaging is a method to measure the diffusion length of free carriers in a semiconductor. The diffusion length is the characteristic distance that free carriers travel before recombination. It is directly related to the mobility-lifetime product of a material. However, in a case where the generation volume due to the incident beam is not small compared to the diffusion length, it is hard to determine the diffusion length by transport imaging because the model for transport imaging does not yet take into account a finite generation region.

Figure 3 JEOL 840A scanning electron microscope (SEM)

In previous work, transport imaging has been used to measure diffusion length for nanowire materials [4] and thin layers of solar cells [5]. To measure the diffusion length of bulk materials is a new challenge. Specifically, a relatively short diffusion length is hard to determine because it is difficult to describe the deposited energy at the center of the material. This effect is particularly critical in bulk samples.

To capture transport imaging, the capability of a SEM and a microscope and a camera with good spatial resolution are needed. This means that the electron beam in a SEM can generate electrons and holes in materials and the generated photons can be imaged by a sensitive camera over the full luminescence spectrum of the material. The absolute intensity of the collected luminescence is not important because the intensity is normalized to compare the results in different conditions. Thus, the exposure time of the camera can be adjusted to get sufficient total signal.

A JEOL 840A SEM is used for transport imaging, which can be seen in Figure 3. In the silver box towards the middle of the figure, there is a vacuum chamber that can hold samples. On the right and left sides of the sample chamber are a Si-CCD camera for imaging and a monochrometer for spectroscopy, respectively.

A. EXPERIMENTAL SETUP

A sample is placed in the vacuum chamber as shown in Figure 4. In the chamber, the electron beam is incident perpendicular to the sample as shown in the schematic of Figure 5. The generated photons are captured by the Si-CCD camera as seen in Figure 6. The resolution of the CCD array on the microscope is 0.4 μm per pixel. The monochrometer shown in Figure 7 is used to measure the spectrum of a luminescent material.

There are three operating modes in the JEOL 840A SEM: spot, line and picture mode. The spot mode focuses the electron beam on one point, while the electron beam moves back and forth quickly along a single line in line mode. Picture mode is used to view large areas of a sample and focus the electron beam. The experiments described in

this thesis are conducted in spot mode because line mode is difficult to calculate by Monte Carlo simulation. For generation at a spot, however, direct comparison to the simulation can be made.

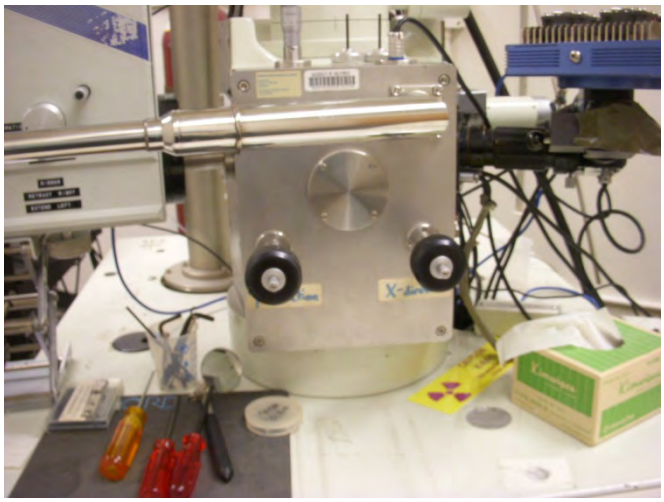

Figure 4 Vacuum chamber on the JEOL 840A SEM

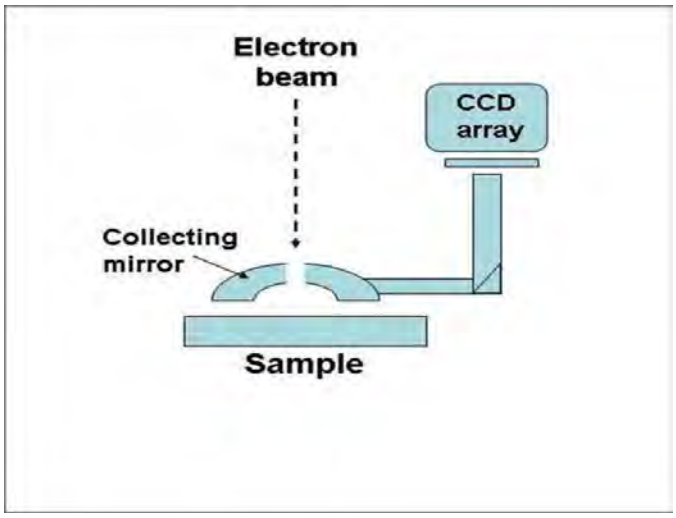

Figure 5 Schematic of the system for generating charge and imaging in the SEM

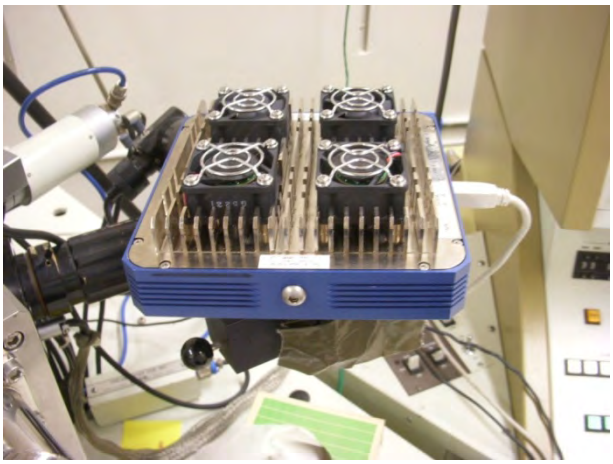

Figure 6 Si CCD camera

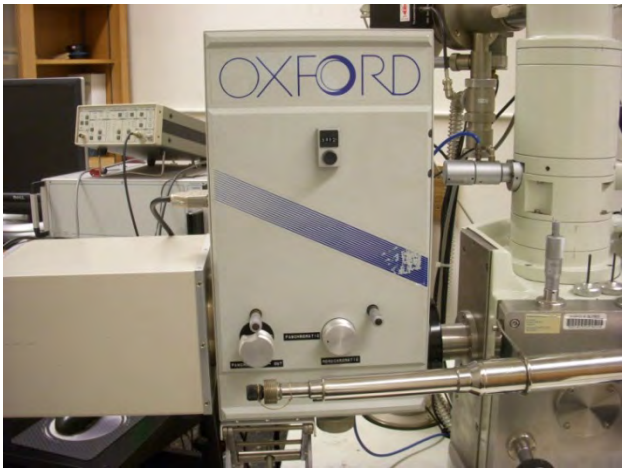

Figure 7 Monochrometer

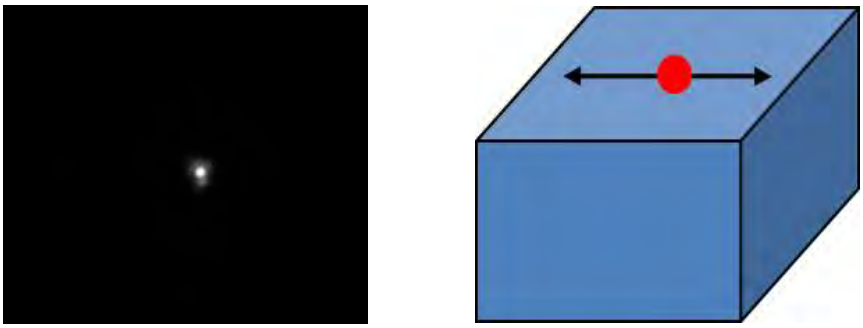

Figure 8 Direct Imaging of CdTe in the SEM spot mode when the incident electron energy is 20 keV with the probe current 3E-10 A

The spot mode optical image of the top surface of a material under spot mode excitation is shown in Figure 8. From the picture, a line through the brightest point in the picture is chosen. Then the data are normalized and plotted as shown in Figure 9 and Figure 10.

B. MEASUREMENTS OF TRANSPORT IMAGING

In the research, cadmium telluride and zinc selenide are selected because they are believed to have small diffusion lengths to enable study of the generation volume. Cadmium telluride is also an important material for room temperature nuclear radiation detectors.

Figure 9 and Figure 10 show the transport imaging distribution for cadmium telluride (CdTe) and zinc selenide (ZnSe) in spot mode at three electron beam energies: 10, 20 and 30 keV. Both cases show that the width of the distribution is near 5 microns. For cadmium telluride, the distribution of photons is different according to the incident electron beam energy. At 30 keV, electron-hole pairs have a broader spatial distribution than at 10 keV. For zinc selenide, the distribution is independent of electron beam energy. Thus, the distribution length does not reflect the diffusion length in the material and there are other factors contributing to the recombination distribution. For cadmium telluride, the generation volume activated by the electron beam plays an important role in the distribution of luminescence but there appear to be other factors affecting the distribution for zinc selenide.

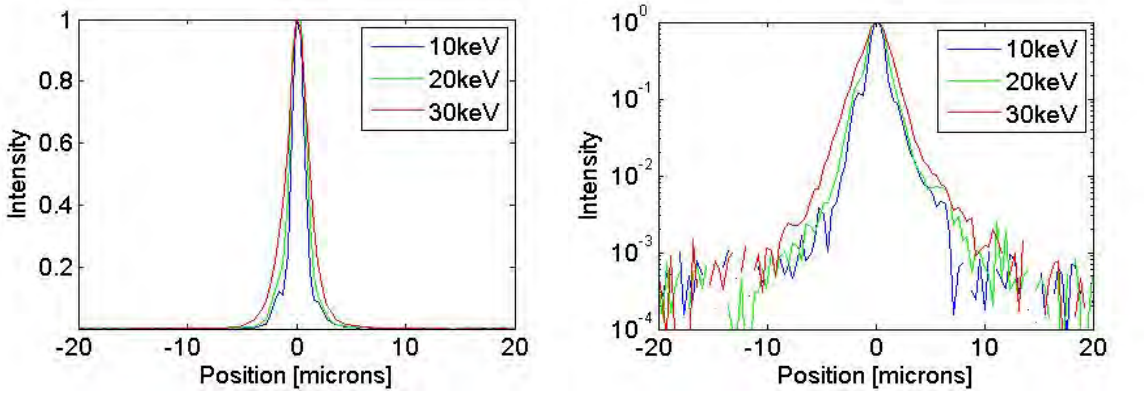

(a) Linear scale (b) Log scale

Figure 9 Luminescence distribution as a function of position for CdTe at 10, 20 & 30 keV with the probe current 3E-10 A

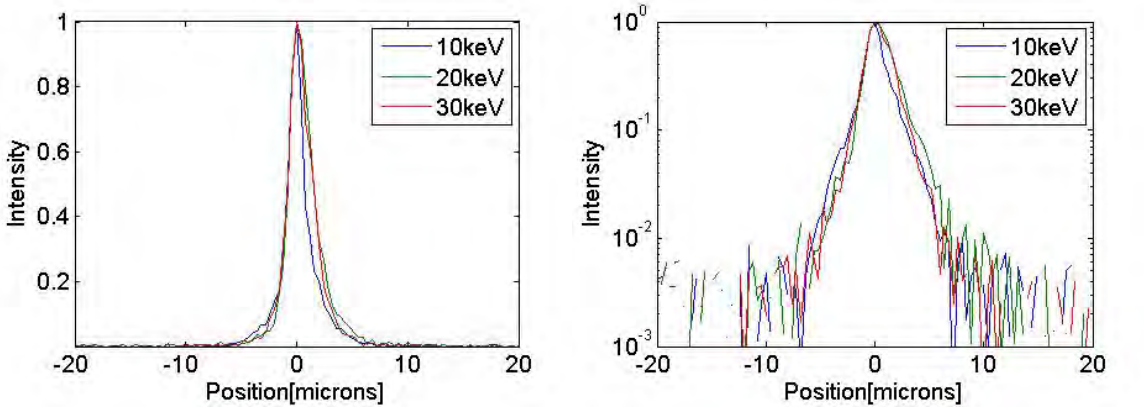

(a) Linear scale (b) Log scale

Figure 10 Luminescence distribution as a function of position for ZnSe at 10, 20 & 30 keV with the probe current 3E-10 A

Figure 11, Figure 12 and Figure 13 show the transport imaging of several other bulk samples, which have different atomic numbers, taken in line mode at 20 keV. There is no linear relationship for different atomic numbers, but cadmium telluride, zinc selenide and gallium arsenide (GaAs) show the smallest spatial distribution of photons. Zirconium oxide (ZrO_2) shows a totally different pattern. This pattern originates either from a relatively large diffusion length compared to other materials or from some another effect. These cases show that transport imaging has limitations for obtaining diffusion

lengths when the diffusion length of photons is relatively small and the materials have various generation volumes. To obtain a reliable diffusion length, other factors that have an effect on transport imaging must be studied.

Material	Atomic Number	Material	Atomic Number
SiC	20	GaAs	64
ZnS	46	ZnSe	64
ZrO_2	56	CdTe	100

Table 1 Sample materials and atomic numbers

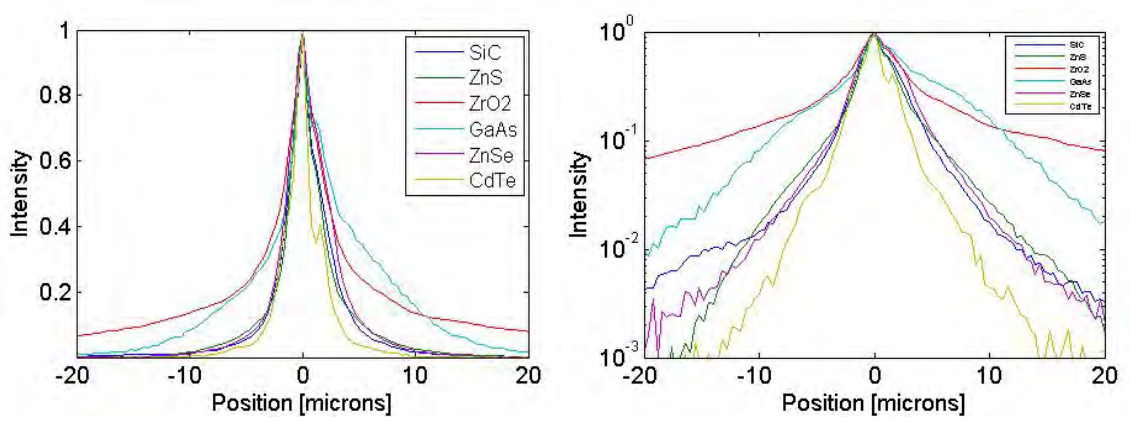

(a) Linear scale (b) Log scale

Figure 11 Luminescence distribution as a function of position for six samples (SiC, ZnS, $Zr0_2$, GaAs, ZnSe & CdTe) at 10 keV with the probe current 3E-10 A

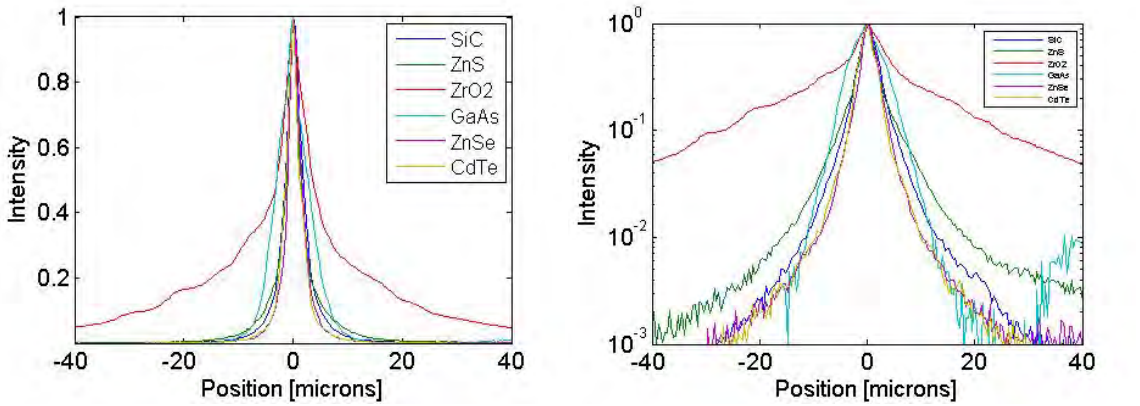

(a) Linear scale (b) Log scale

Figure 12 Luminescence distribution as a function of position for six samples (SiC, ZnS, $Zr0_2$, GaAs, ZnSe & CdTe) at 20 keV with the probe current 3E-10 A

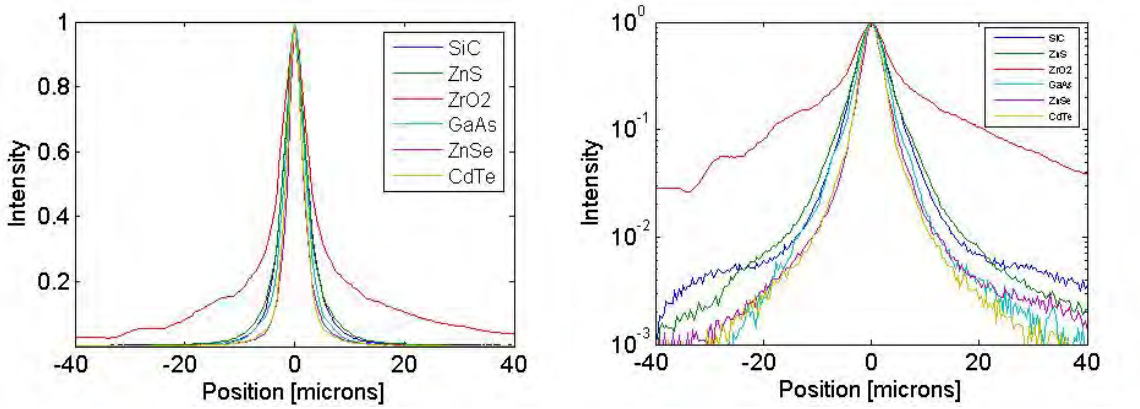

(a) Linear scale (b) Log scale

Figure 13 Luminescence distribution as a function of position for six samples (SiC, ZnS, $Zr0_2$, GaAs, ZnSe & CdTe) at 30 keV with the probe current 3E-10 A

As previously mentioned, transport imaging is limited in determining the diffusion length of a material when the distribution of photons is small and the generation volume varies due to materials and electron beam energy. In the next chapter, the relationship between transport imaging and the generation volume simulated by Monte Carlo software is discussed. Furthermore, an additional factor that could have an effect on transport imaging will be discussed.

III. MONTE CARLO SIMULATION FOR ELECTRON-SOLID INTERACTION

Monte Carlo simulation is widely used to understand the interaction between incident electrons and samples in the Scanning Electron Microscope. This simulation calculates elastic and inelastic scattering in a material when an electron beam of a given energy interacts with the material. Elastic scattering means that electrons are scattering off the nuclei of a material and change the direction of travel randomly while inelastic scattering occurs when incident electrons interact with electrons in the valence band, lose energy, and, in some cases, make electron-hole pairs in the material. In other words, elastic scattering determines only the electron trajectories while inelastic scattering also deposits energy in the volume of the semiconductor and generates electrons and holes [6]. In Monte Carlo simulations, electrons penetrate a material by having both elastic and inelastic scattering events. The trajectory of each electron is determined randomly. When this process is repeated many times, the simulation shows a reproducible result for the energy distribution in a target material.

For this research, one version of Monte Carlo Simulation software, CASINO, Monte **CA**rlo **SI**mulation of electro**N** trajectory in s**O**lid, was used. This program was developed by the scientific community at the Usherbrooke University in Canada. They provide this program on their website [7] freely and recently released the latest version of the program, CASINO Version 3.2. In the beginning of my research, the previous version of CASINO (ver. 2.4) was used. However, ver. 2.4 cannot calculate the secondary electron trajectories, so the new version was utilized at the end of the research. There are several modifications between old and new CASINO, but the primary capability in the software is the same. The new version mainly provides the additional function to calculate secondary electron trajectories.

A secondary electron means that incident electrons from an incident electron beam scatter from valence electrons in the solid and give kinetic energy to electrons in the material. These electrons are secondary electrons which act like primary electrons but have less energy than the primary. Figure 14 shows the difference in energy distribution

when secondary electrons are included in the simulation. After normalization, the two cases look almost the same. It means that when secondary electrons are calculated, additional energy is deposited in a material but the size of the activated volume is almost the same.

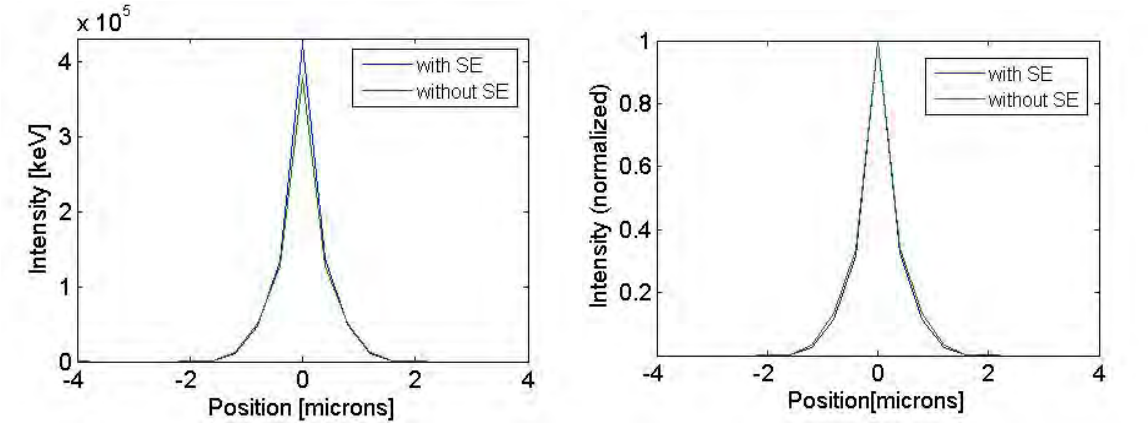

(a) Before normalization (b) After normalization

Figure 14 Distribution of deposited energy as a function of position with and with calculation of secondary electron effect for ZnSe at 20 keV in the simulation

A. CACULATION SETUP

To get reliable data, the number of electron trajectories is crucial. Figure 15 shows the energy distribution in gallium arsenide for a different number of electron trajectories. In Figure 15, the upper figures show electron trajectories, and the lower figures show energy distribution in a material. As the electron beam is perpendicular to a material's surface, the energy distribution for a large number of trajectories should be symmetric in the plane. The left simulation has 100 incident electrons and the right simulation has 100,000 incident electrons. As is shown, the right side one is the most symmetric. Thus, the software should be simulated for at least 100,000 electrons to obtain reliable spatial data.

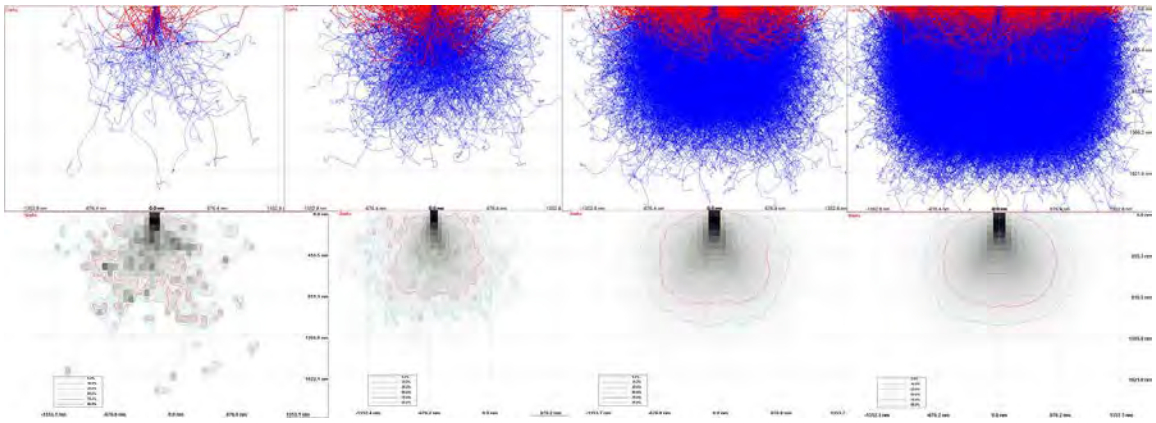

(a) 100 times (b) 1,000 times (c) 10,000 times (d) 100,000 times

Figure 15 CASINO calculation in GaAs for increasing number of incident electrons: top parts are electron trajectories and lower parts are deposited energy densities.

To compare the simulations to the result of transport imaging, the parameters for the CASINO calculation are matched to the setting of SEM. The electron beam radius on the surface is 56 nm [8]. For the electron's trajectory simulation, the Kanaya Okayama model is selected. The Kanaya Okayama model is a model of electron penetration into an amorphous solid, related to the maximum energy dissipation depth and range based on a modified Thomson-Whiddington law and the Lenard absorption law [6]. To compare the results, the pixel size should be matched to what can be observed with the CCD camera, so 0.4 microns per pixel is used in CASINO calculation. The density of a material is automatically calculated based on each element's density and weight fraction. For example, when the values for gallium (atomic number (Z) and density (d)) are 31 and 5.91 g/cm^3 and arsenic (Z and d) are 33 and 5.72 g/cm^3, the density of gallium arsenide is presented as 5.81 g/cm^3. While the user of this software can input a specific number for his or her sample, the author applied the calculated value in the program. To generate secondary electrons, the work function and the plasmon energies are needed [9]. The author estimated the work function and the plasmon energies of materials as the mean of each value of materials, which are given in the software, except for the gallium arsenide plasmon energy as shown in Table 2.

Material	Density(g/cm^3)	Work function (eV)	Plasmon Energy (eV)
SiC	2.4099	4.925 (Si: 4.85, C: 5)	25.25 (Si:16.5, C: 34)
ZnS	3.9538	N/A (Zn: 4.9, S: N/A)	N/A (Zn: 17.8, S: N/A)
ZrO_2	3.3807	N/A (Zr: 4.05, O: N/A)	N/A (Zr: -1, O: N/A)
GaAs	5.81	3.975 (Ga: 4.2, As: 3.75)	15.8 (given in software)
ZnSe	5.6368	5.4 (Zn: 4.9, Se: 5.9)	18.4 (Zn: 17.8, Se: 18.9)
CdTe	7.1765	4.585 (Cd: 4.22, Te: 4.95)	18.15 (Cd: 19.2, Te: 17.1)

Table 2 Sample materials and Input parameters for Monte Carlo simulations

The energy of electrons when the simulation is terminated is also an important setting for the simulation. At this energy, electrons are assumed to stop their travels in a material. However, "stopped" electrons still have enough energy to generate inelastic scattering, which means additional electron-hole pairs. The developer recommends that more than 50 eV be used because the physical models in the software are not accurate below 50 eV [10]. In Figure 16, when the stopped electrons' energy level is set to 10 eV, the generation volume is basically the same as when the level is 50 eV. In the case of 10 eV, the calculation time is much longer than 50 eV, but the results are similar. As a result, 50 eV is utilized as the stopped electron energy in the research.

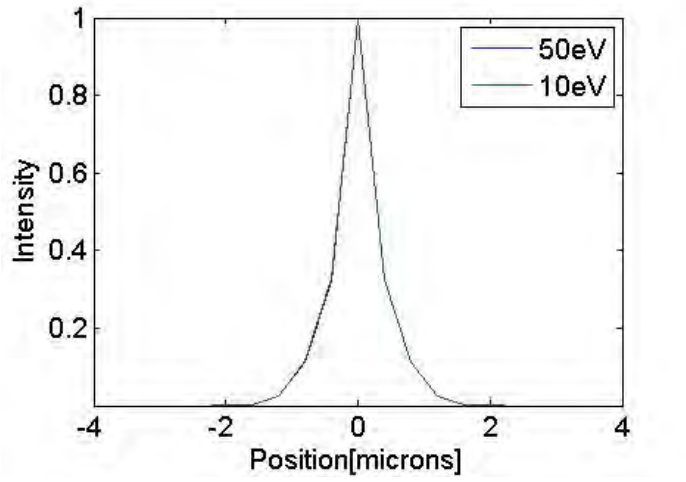

Figure 16 Comparison when the stopped electron energy is 50 eV and 10 eV in ZnSe

Using this setup, the program calculates the electron trajectories and the deposited energy density in a material. Figure 17 is the result of CASINO Monte Carlo software for silicon carbide with 20 keV incident electrons. On the left side, the simulation of electron

trajectories is presented. The cube is silicon carbide as a bulk material, the blue beam on the top of the surface is an electron beam and random curves in the cube indicate e lectron trajectories. The green curves present the trajectories of secondary electrons. In the right upper side, the energy density in the silicon carbide on the xy-plane is shown and the right lower one is for the x-z plane.

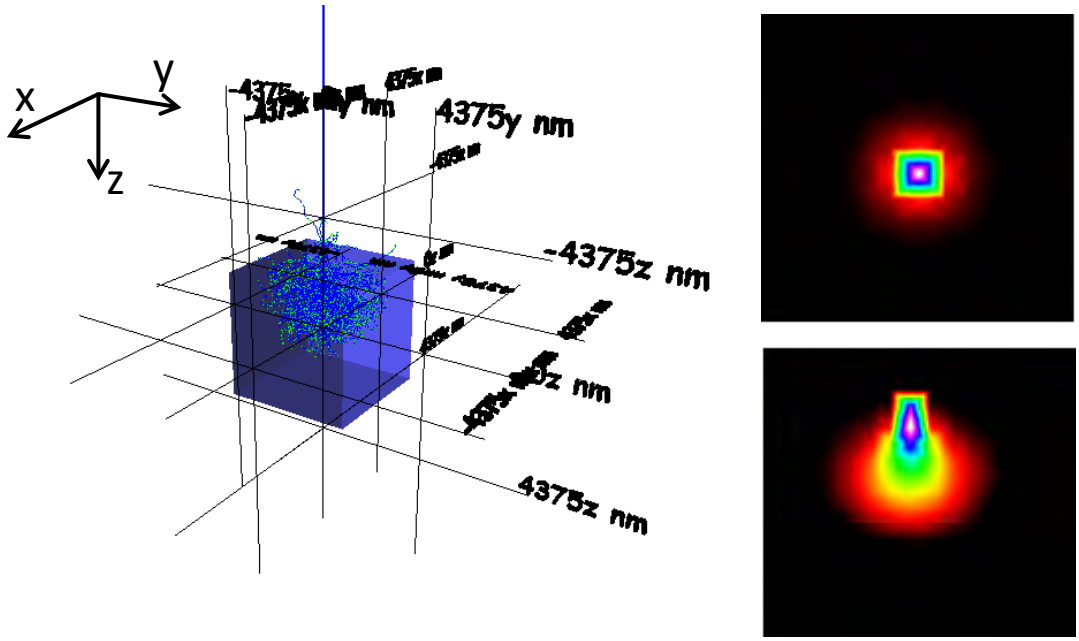

Figure 17 CASINO Image of generation volume in SiC for 20 keV incident electrons. Left is the simulation of electron trajectories in the material. Right (top) is the energy density on the xy-plane and right (bottom) is the energy density for the x-z plane.

B. CALCULATION OF GENERATION VOLUME

In order to compare direct optical imaging in the SEM and the energy density from the CASINO simulation, the distribution of energy density is converted to the same format as the data of direct optical imaging, which means that the same pixel size (0.4 x 0.4 microns) and spatial data in x only are used. The pixel size of the CASINO data is determined by the mesh size of the program, and to make one-dimensional data, the x-z plane, including the point of incident electrons, is chosen as shown as Figure 18. Then the values in the x-z plane are summed along the z-axis. Finally the data are normalized to

the peak height. Figure 19 and Figure 20 show the distributions of the energy densities in cadmium telluride and zinc selenide at 10, 20 and 30 keV as simulated by the CASINO software.

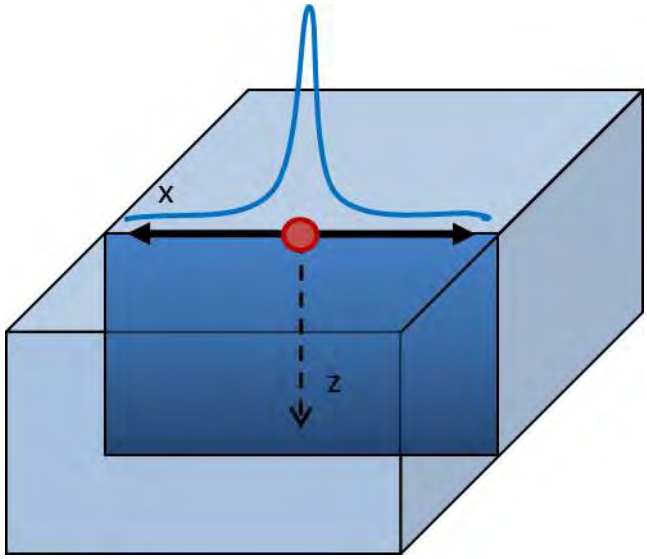

Figure 18 Schematic of formatting of the CASINO data

In all cases of the simulation, when the incident electron energy is increased, the generation volume gets larger. The incident electrons of higher energy travel further into a material, so the generation volume is larger, which means that the primary distribution of electron hole pairs is larger in all directions. This definitely plays a role in the direct optical imaging. In Figure 19 and Figure 20, one sees the increase in generation volume with increasing energy of the incident electrons.

For a fixed energy for the incident electrons, the width of the energy density is dependent on the density of material. Figure 21 shows the distribution of the energy density for six samples with the same energy of incident electrons. The spatial variation in the energy distribution is the same order as the density variation of the materials, which are given in Table 2. Thus, the generation volume of a material is inversely proportional to the density of a material. High density means that the distance between atoms gets shorter and the atoms are more effective scattering sites, so more scattering occurs in the same volume when the density gets higher. In other words, more elastic and inelastic events occur with incident electrons and the trajectories of electrons are shorter

as shown in Figure 21. Thus, in a material with large density, the generation volume should have less effect on the direct optical imaging than in a material with small density.

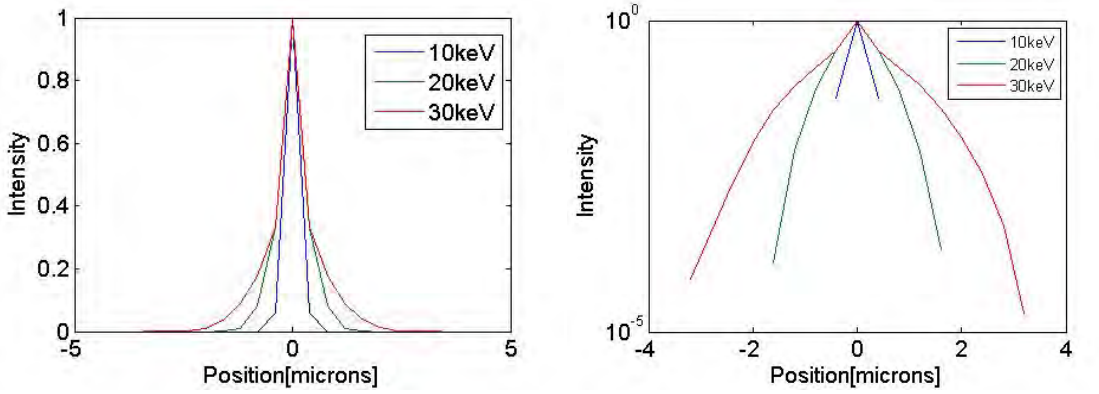

(a) Linear scale (b) Log scale

Figure 19 Distribution of energy density in CdTe for 10, 20 & 30 keV incident electrons

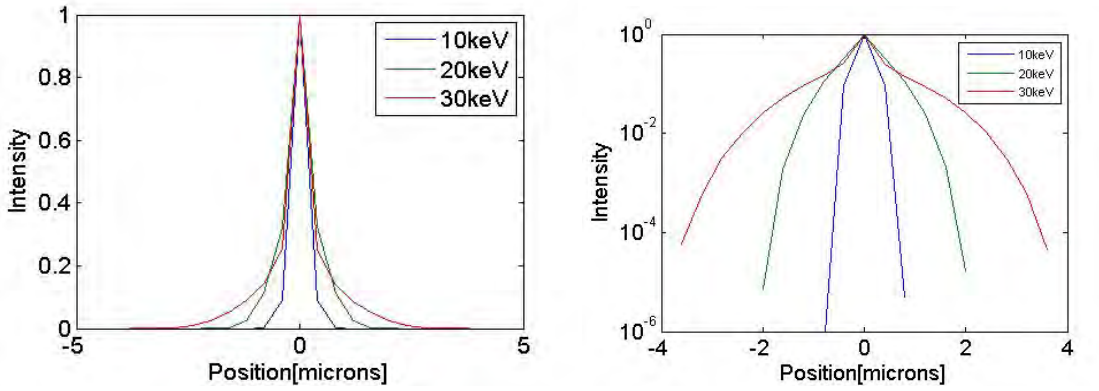

(a) Linear scale (b) Log scale

Figure 20 Distribution of energy density in ZnSe for 10, 20 & 30 keV incident electrons

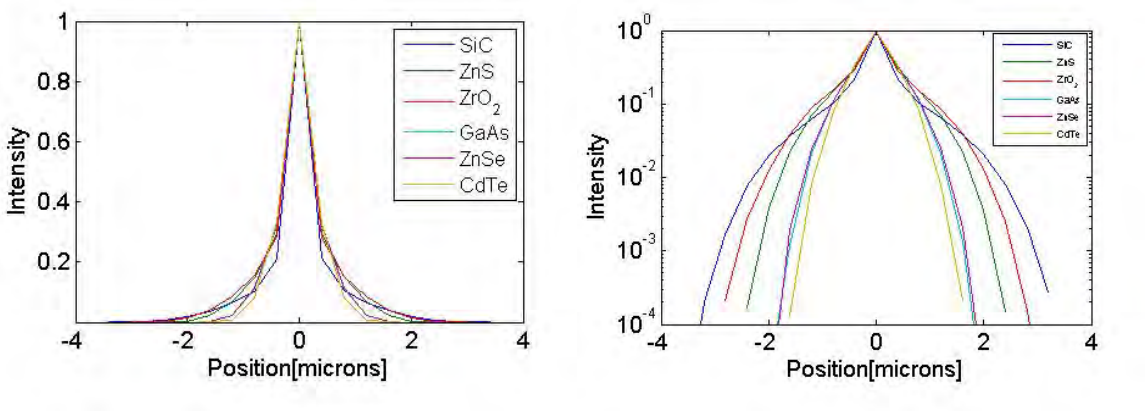

(a) Linear scale (b) Log scale

Figure 21 Distribution of energy density in six different materials for 20 keV incident electrons

C. COMPARISON WITH TRANSPORT IMAGING

Clearly, density of the material and the energy of incident electrons play an important role in determining the generation volume. A higher incident energy results in a larger generation volume, and a larger density of a material makes the generation volume small. For the direct optical imaging, however, these relationships are not applicable for all materials. In cadmium telluride, the difference of energy density can explain the difference in direct optical imaging for 10, 20, 30 keV. In Figure 22, when the generation volume gets larger due to the incident energy, 10, 20 and 30 keV, the direct imaging distribution also becomes larger. The difference in the distributions between both stays fairly constant, so the difference is assumed to reflect the diffusion length in cadmium telluride as shown in Table 3.

Incident Electron Energy	**Width of imaging [microns]**		**Difference btween DI & GV** [microns]
	Direct Imaging	Generation Volume	
10 keV	8.8	0.8	8.0
20 keV	12	3.2	8.8
30 keV	14	6.4	7.6

Table 3 Difference of the size between the direct imaging and the generation volume in CdTe at the incident energy 10, 20 & 30 keV

Incident Electron Energy	**Width of imaging [microns]**		**Difference btween DI & GV** [microns]
	Direct Imaging	Generation Volume	
10 keV	18.0	1.6	16.4
20 keV	19.0	4.0	15.0
30 keV	20.0	7.2	12.4

Table 4 Difference of the size between the direct imaging and the generation volume in ZnSe at the incident energy 10, 20 & 30 keV

However, in the case of zinc selenide, there is no relationship between the generation volume and the direct imaging distribution as shown in Table 4. In Figure 23, the generation volume becomes larger when the incident energy increases, but the direct imaging is independent of the incident electron energy. The generation volume is one of the factors for the direct optical imaging, and the diffusion length of zinc selenide is not large enough to ignore the generation volume with respect to transport imaging. However, there may be another factor which can also affect the direct imaging of materials. The author assumes that one of the factors to impact on the direct imaging may be a photon-recycling effect. The next chapter discusses this effect.

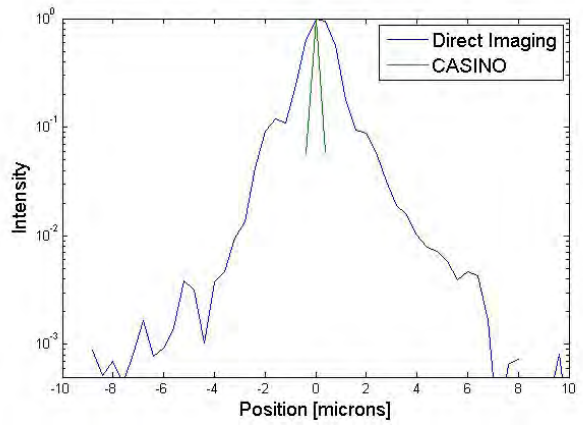

(a) 10 keV

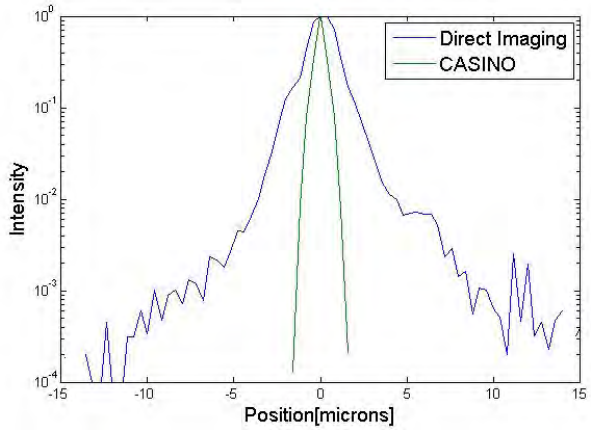

(b) 20 keV

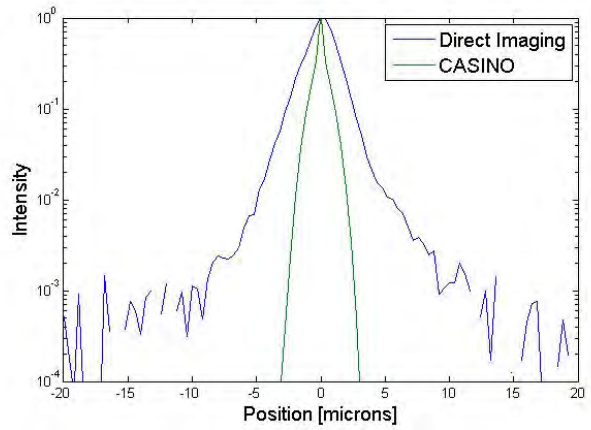

(c) 30 keV

Figure 22 Comparison of the direct imaging and the generation volume in CdTe at the incident energy 10, 20 and 30 keV

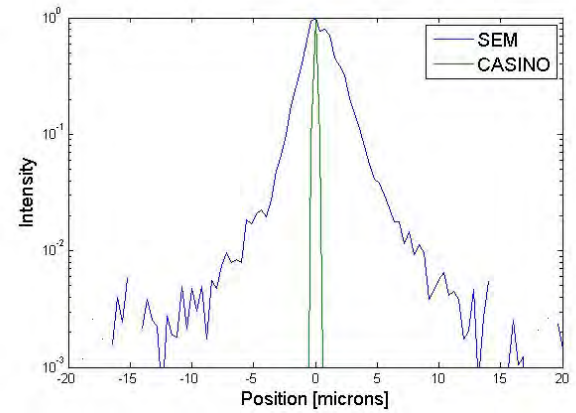

(a) 10 keV

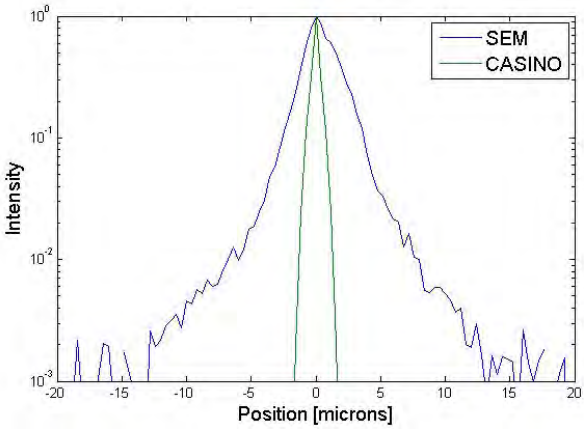

(b) 20 keV

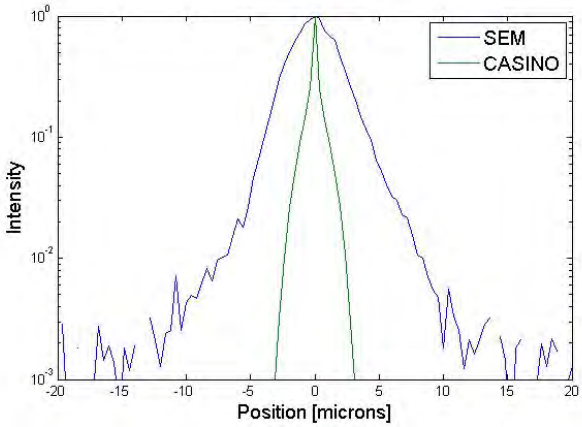

(c) 30 keV

Figure 23 Comparison of the direct imaging and the generation volume in ZnSe at the incident energy 10, 20 and 30 keV

THIS PAGE INTENTIONALLY LEFT BLANK

IV. PHOTON RECYCLING EFFECT

The “photon recycling effect” is defined as the process through which photons of shorter wavelength propagate and are reabsorbed to produce longer wavelength photons at a different location in a material. In a SEM, incident electrons generate photons from electron-hole pairs recombining in a material. Depending on the type of luminescence from the material, these photons can produce longer wavelength photons as depicted schematically in Figure 24. Photons which have the highest energy will generate lower energy photons further out in the material. Many materials luminesce both at the band edge energy and also at lower energies depending on dopants and defects.

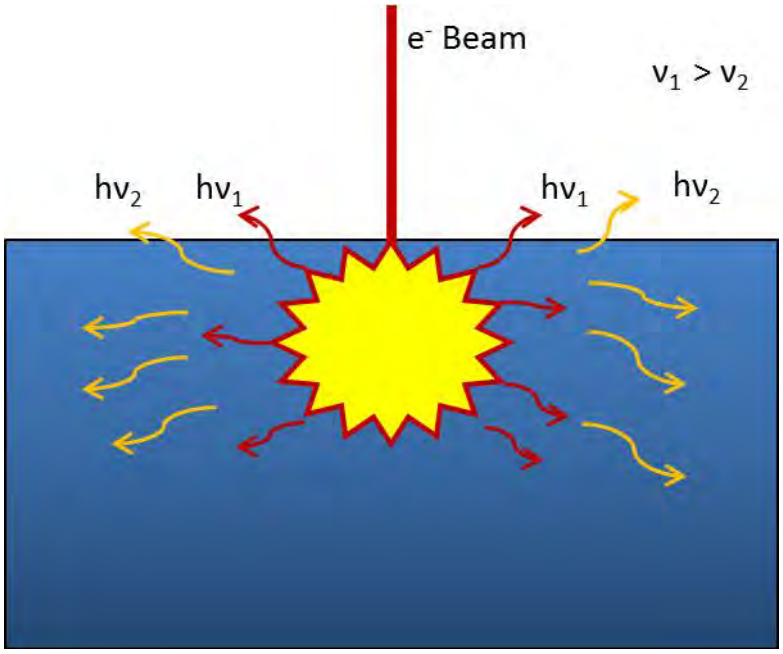

Figure 24 Schematic of photon recycling effect

To measure the photon recycling in a material, the full emission spectrum needs to be determined. In the spectra measured by the cathodoluminescent (CL) spectroscopy shown in Figure 7, one or two peaks are generally observed. Figure 25 shows the spectra from 300 nm to 900 nm for a range of sample materials. Table 5 summarizes the distinct

peak wavelength in all materials. Two materials have two peaks in their spectrum: zinc sulfide and zinc selenide. Therefore, these two materials are chosen for the experiment on the photon recycling effect.

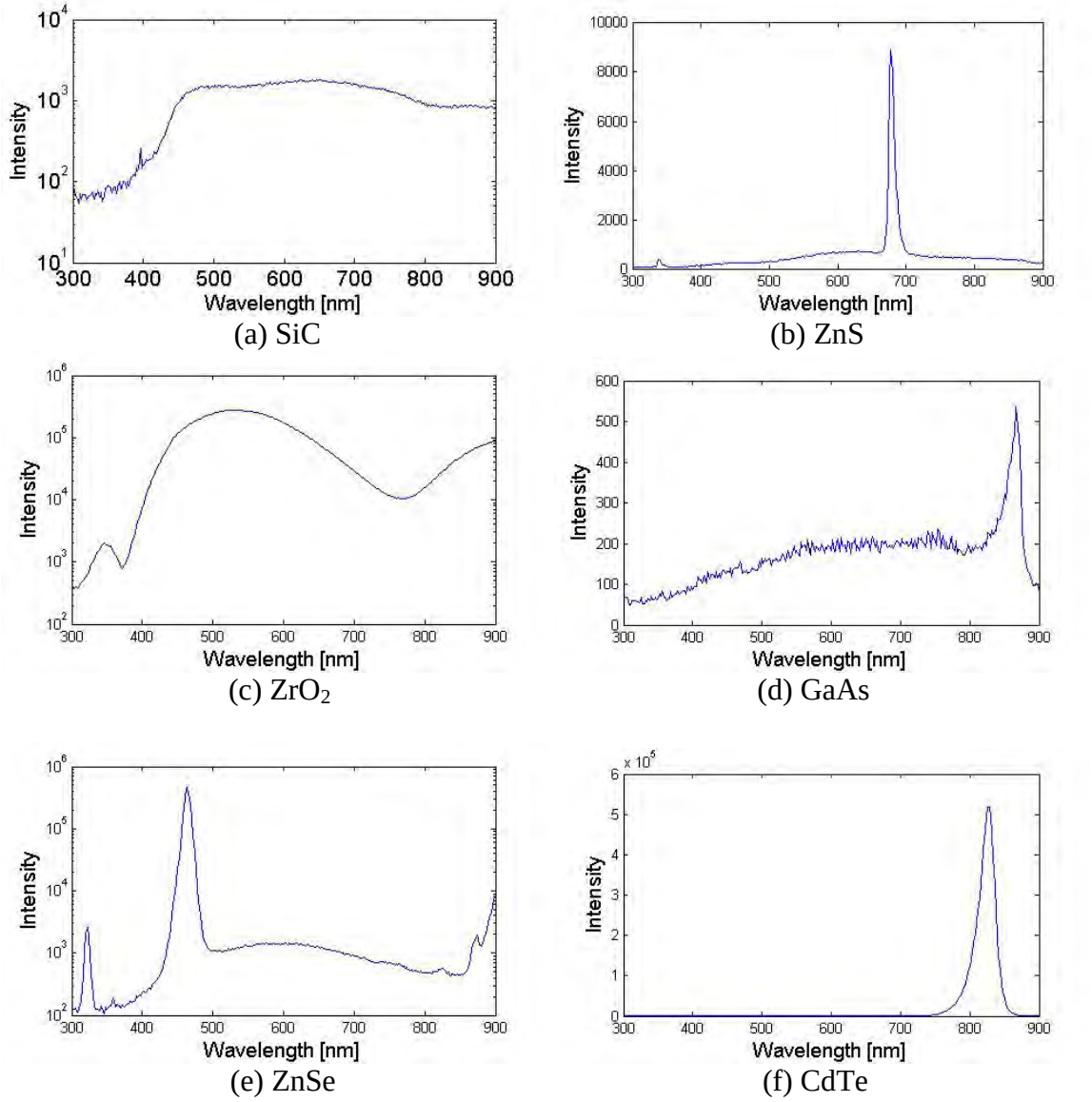

Figure 25 Cathodoluminescence spectra of 6 samples. Note: The figures on the left are plotted on a log scale to highlight the peaks. The figures on the right are plotted on a linear scale.

Material	Peak Wavelength	Material	Peak Wavelength
SiC	400 nm	GaAs	870 nm
ZnS	340 & 690 nm	ZnSe	320 & 470 nm
ZrO_2	350 nm	CdTe	870 nm

Table 5 Sample materials and peak luminescence wavelengths

In order to attempt to isolate the photon recycling effect, a band-pass filter for the shortest wavelength in a material and a long-pass filter for secondary generated photons are used. With a band-pass filter, we expect the intensity to be much smaller than without the filter, but also to see potentially a much narrow distribution. With a long-pass filter, the intensity will also be reduced, though not as dramatically, but the distribution width should remain the same. Because all data are normalized for comparison, these results might show a different width at the same incident energy if photon recycling is playing a role.

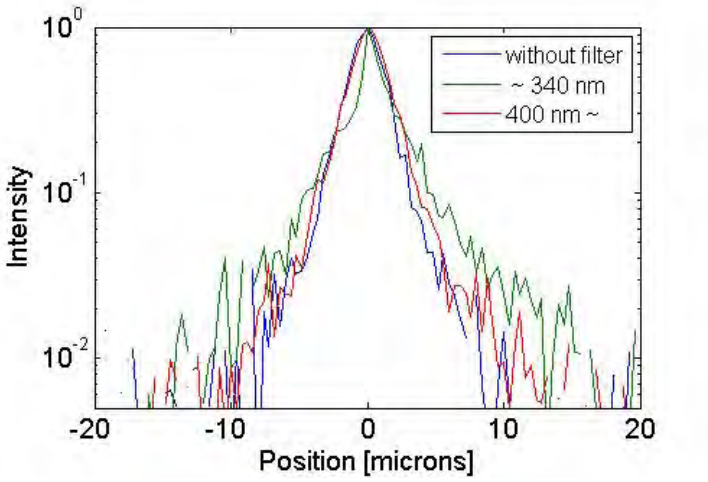

Figure 26 Direct imaging in ZnS at 20 keV without filters, with a band-pass filter and with a long-pass filter with the probe current 1E-9 A

In the case of zinc sulfide, three different direct images were taken. One is the direct imaging at 20 keV electron beam energy without any filter. The next one is for the first peak wavelength with a band-pass filter of 335 - 345 nm. The final one is for longer wavelengths than the first peak with a long-pass filter of 400 - 900 nm. Figure 26, however, shows no difference among these results. This is because the second peak of

zinc sulfide is located at the twice the wavelength of the first peak wavelength. That means that the second peak of zinc sulfide is most likely a second order diffraction effect.

For zinc selenide, there are also two distinct peaks in the spectrum. The author utilized the same filter approach for zinc sulfide. However, direct imaging with a band-pass filter of 315 - 325 nm was not sufficient to produce a signal in the Si-CCD camera. There are two reasons: the reflectivity of the band-pass filter is 40 %, and the sensitivity of the CCD camera at 315 - 325 nm is less than 20% as shown in Figure 27. To take the direct imaging with the band-pass filter, another detector which has more sensitivity for near UV will be needed.

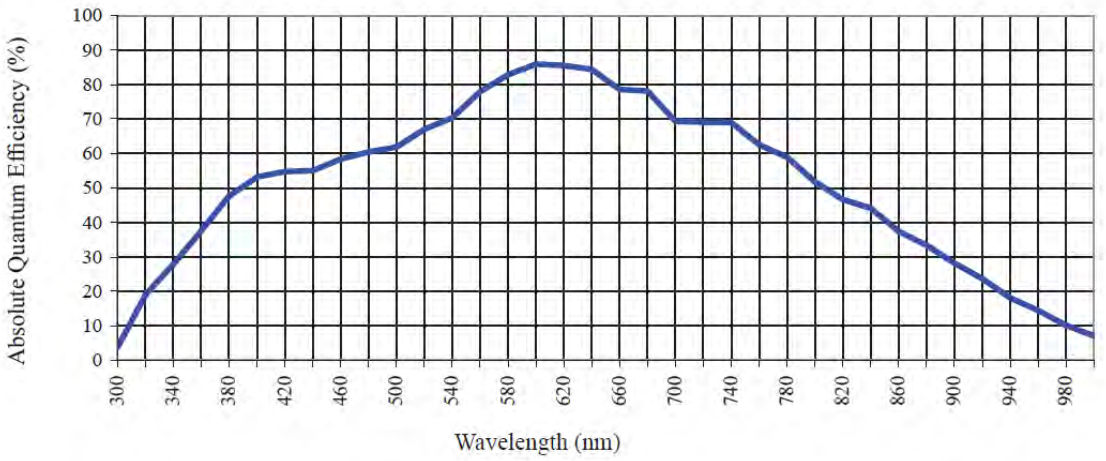

Figure 27 CCD camera sensitivity. From [11].

V. CONCLUSIONS AND AREAS FOR FUTURE RESEARCH

A. CONCLUSIONS

To determine the diffusion length which leads to the mobility-lifetime product of a material, transport imaging is a promising method. However, for relatively short diffusion lengths, the direct optical imaging of a material is affected by the generation volume produced by the electron beam in SEM. To understand this effect, Monte Carlo simulations were performed. By performing the simulations for a range of materials, we show that the generation volume is larger when the energy of incident electrons becomes bigger. For a given energy of the electron beam, the generation volume is dependent on the density of the material. The material that has a larger density shows a small generation volume as shown in Figure 21. As a result, the density of the material plays a key role in determining the generation volume for a material.

Transport imaging is affected by the generation volume when diffusion lengths are small. For cadmium telluride, when the generation volume becomes larger due to higher incident energy, the direct transport imaging also gets larger. Furthermore, the difference between the generation volume and the direct imaging is quite uniform as shown in Table 3. In this case, the density of cadmium telluride is relatively large compared to other samples, so the generation volume has less of an effect on the direct imaging. However, the diffusion length is not very large as compared with the generation volume, so the generation volume of cadmium telluride affects the direct imaging uniformly.

On the other hand, for zinc selenide, the generation volume is still dependent on incident energy, but experimentally transport imaging of zinc selenide is independent of beam energy. This suggests that there is another factor in the direct imaging of zinc selenide. In this research, the photon recycling effect is proposed to play a role for a case of zinc selenide. The effect of photon recycling could not be determined in this research because of the limitation of the sensitivity of the CCD camera and the low transmission of the band-pass filter.

B. FUTURE WORK

The Monte Carlo simulation of electron interactions in solids in the SEM can provide a lot of useful data. For example, the trajectory length of electrons along the z-axis, called Z-max in CASINO, can provide z_0 to apply in the model for transport imaging, where z_0 is the average depth of the generation region as shown in Figure 28 [12]. Thus, further research is needed to define the relationship between Z-max and z_0. A second example is the position of stopped electrons in the x and y plane. This distribution shows the size of the generation volume of a material. Because the top surface of a material is observed in SEM, the x and y positions of stopped electrons would be useful to more fully understand the generation volume created by the electron beam.

In addition, the community that developed the CASINO Monte Carlo simulation is focusing on the simulation of the cathodoluminescence [7]. At this time, researchers are writing an article concentrating on the simulation of the cathodoluminescence, which will finally address the relationship between energy deposition and electron-hole pair generation that is needed for understanding optical effects.

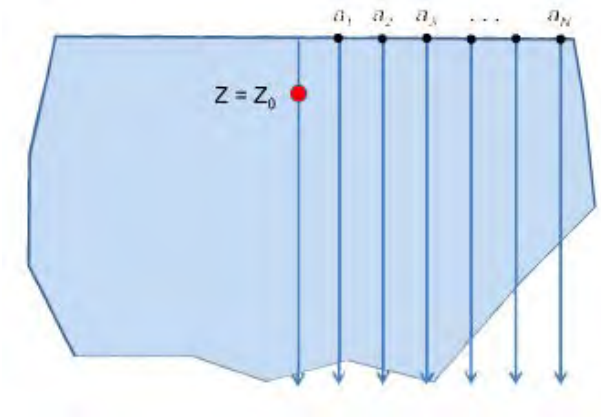

Figure 28 Determining z_0 for the model of the transport imaging. From [12].

For cadmium telluride, the appropriate model is available to combine the direct imaging and the generation volume. To be improved to accommodate shorter diffusion lengths, the model should include an empirical description of the generation volume. By using the result calculated by CASINO, the new model for cadmium telluride will be developed.

LIST OF REFERENCES

[1] A. V. Churilov et al., "Thallium bromide nuclear radiation detector development," *IEEE Transactions on Nuclear Science*, vol. 56, no 4., Aug. 2009.

[2] T. E. Schlesinger and R. B. James, "Semiconductors for Room Temperature Nuclear Detector Applications," *Semiconductors and Semimetals*, vol. 43, pp. 2–11, 1995.

[3] N. M. Haegel et al., "Imaging transport for the determination of minority carrier diffusion length," *Applied Physics Letters* 88, 2006.

[4] L. Baird et al., "Transport Imaging for Contact-free Measurements fo Minority Carrier Diffusion in GaN, GaN/AlGaN, and GaN/InGaN cour-shell nanowires," *Applied Physics Letter*, vol. 98, 2011.

[5] N. M. Haegel, T. Mills, M. Talmadge, C. Scandrett, C. Frenzen, H. Yoon, C. Fetzer, and R. King, "Direct imaging of anisotropic minority-carrier diffusion in ordered gainp," *Journal of Applied Physics*, vol. 105, no. 2, pp. 023711–023711, 2009.

[6] K. Kanaya and S. Okayama, "Penetration and energy-loss theory of electrons in solid targets," *Appl. Phys.,* vol. 5, 1972.

[7] Casino, Universite de sherbrooke, "Monte Carlo, simulation of electron trajectory in solids," November 2011, http://www.gel.usherbrooke.ca/casino /index.html.

[8] R. Cole, "Near field imaging of charge transport in gallium nitride and zinc oxide nanostructures," M.S. thesis, Naval Postgraduate School, December 2010.

[9] H. Demers et al., "Three-dimensional electron microscopy simulation with the CASINO Monte Carlo software," *Scanning*, vol. 33, 2011.

[10] D. Drouin et al., "CASINO V2.42—A fast and easy-to-use modeling tool for SEM and microanalysis users," *Scanning* vol. 29, 92–101, 2007.

[11] Apogee imaging systems, "High performance cooled CCD camera system ALTA U32," November 2011, http://www.ccd.com/pdf/U32.pdf.

[12] K. Blaine, "Contact free measurement of mobility-lifetime product using transport imaging," M.S. thesis, Naval Postgraduate School, June 2011.

THIS PAGE INTENTIONALLY LEFT BLANK

INITIAL DISTRIBUTION LIST

1. Defense Technical Information Center
   Ft. Belvoir, Virginia

2. Dudley Knox Library
   Naval Postgraduate School
   Monterey, California

3. Dr. Nancy Haegel
   Naval Postgraduate School
   Monterey, California

4. Dr. Peter Crooker
   Naval Postgraduate School
   Monterey, California

5. Headquarter of Army, Library
   Republic of Korea Army
   Gyeryoung, Republic of Korea

6. Korea National Defense University, Library
   Goyang, Republic of Korea

7. Maj. Yoseoph Seo
   Korea National CBRND Command
   Seoul, Republic of Korea